AAEC/E380

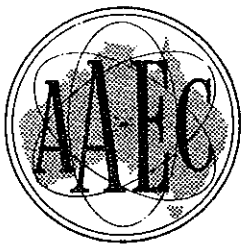

AAEC/E380

AUSTRALIAN ATOMIC ENERGY COMMISSION

RESEARCH ESTABLISHMENT

LUCAS HEIGHTS

THE PROMPT NEUTRON DECAY CONSTANT OF THE MOATA REACTOR AND RELATED COUPLED-CORE ASSEMBLIES

by

R.B. KNOTT
J.R. HARRIES

March 1976

ISBN 0 642 99741 1

AUSTRALIAN ATOMIC ENERGY COMMISSION
RESEARCH ESTABLISHMENT
LUCAS HEIGHTS

THE PROMPT NEUTRON DECAY CONSTANT OF THE MOATA REACTOR AND RELATED COUPLED-CORE ASSEMBLIES

by

R.B. Knott
J.R. Harries

ABSTRACT

The correlation functions of the neutron noise have been used to determine the prompt neutron decay constant, α, for the AAEC reactor Moata - a Universities' Training Reactor (UTR). The basic characteristics of the UTR system are two coupled ^{235}U fuel cores, hydrogen moderated and graphite reflected. To investigate this type of reactor in greater detail, a series of 'mockup' assemblies was constructed on the AAEC Split-table Zero-power Critical Facility. A value of α was experimentally determined for each assembly, and the effects on α of core separation, fuel arrangements, perturbations to the coupling region, and detector positions were investigated. A comparison with previous results for the Moata reactor and with results for similar UTR systems was carried out.

Using a two-dimensional neutron diffusion and kinetics computer code, the prompt neutron generation time, Λ, and the effective delayed neutron fraction, β, were calculated for each assembly. The results from the two-dimensional calculations were consistent with experiment, but the difficulty of modelling the neutron leakage limited the accuracy of the calculated α. Improved agreement with experiment was obtained using a three-dimensional diffusion calculation.

National Library of Australia card number and ISBN 0 642 99741 1

The following descriptors have been selected from the INIS Thesaurus to describe the subject content of this report for information retrieval purposes. For further details please refer to IAEA-INIS-12(INIS: Manual for Indexing) and IAEA-INIS-13 (INIS: Thesaurus) published in Vienna by the International Atomic Energy Agency.

COMPARATIVE EVALUATIONS; CORRELATION FUNCTIONS; COUPLED REACTOR CORES; DECAY; MOATA REACTOR; NEUTRON DIFFUSION EQUATION; PROMPT NEUTRONS; REACTOR NOISE; REACTOR SIMULATORS; THREE-DIMENSIONAL CALCULATIONS; TWO-DIMENSIONAL CALCULATIONS; ZERO POWER REACTORS

CONTENTS

1. INTRODUCTION

The analysis of the fluctuations in the neutron population of a zero-power reactor provides information about the kinetic parameters of the reactor. A basic integral parameter is the 'prompt neutron decay constant', α, and for a critical system $\alpha_c = \beta/\Lambda$, where β is the effective delayed neutron fraction and Λ the prompt neutron generation time. In a graphite reflected reactor the generation time, and hence α, depends markedly on the neutron balance in the reflector because of the much longer lifetime in the graphite compared to the fuel region. Consequently, the comparison of a calculated α with experiment is a sensitive test for the adequacy of the theoretical model at the core-reflector interaction.

The correlation functions of the neutron noise have been measured for a series of two-core reactor systems with graphite coupling and reflector regions.

2. CORRELATION FUNCTIONS - THEORY

The output signal from a pulse neutron detector consists of a mean countrate, $\langle n \rangle$, and a superimposed fluctuating component, $n(t)$. The auto-correlation function of the fluctuating component at detector 1 is given by

$$R_{11}(\tau) = \lim_{T \to \infty} \frac{1}{T} \int_0^T [n_1(t) - \langle n_1 \rangle][n_1(t+\tau) - \langle n_1 \rangle]\, dt \quad , \qquad (1)$$

and the cross-correlation function between the fluctuating components from two different detectors 1 and 2 is given by

$$R_{12}(\tau) = \lim_{T \to \infty} \frac{1}{T} \int_0^T [n_1(t) - \langle n_1 \rangle][n_2(t+\tau) - \langle n_2 \rangle]\, dt \quad . \qquad (2)$$

The following theoretical expressions for the auto- and cross-correlation functions can be derived from the point reactor model:

$$R_{11}(\tau) = \varepsilon_1 F \left[\overline{q^2}\, \delta(\tau) + f\varepsilon_1 \chi\, \bar{q}^2 \sum_p A_p G(s_p) \exp\left[-s_p|\tau|\right] \right] \quad , \qquad (3)$$

$$R_{12}(\tau) = \varepsilon_1 \varepsilon_2 F \chi\, \bar{q}^2 \sum_p A_p G(s_p) \exp\left[-s_p|\tau|\right] \quad , \qquad (4)$$

where A_p and s_p are the coefficients and roots of the reactor transfer function G(s) expressed in the form

$$G(s) = \sum_{p=0}^{6} \frac{A_p}{s+s_p} \quad .$$

Further, F is the fission rate in fissions per second, ε_1 and ε_2 are the detector efficiencies in counts per fission, q is the charge released per neutron detected, f is the spatial correction form-factor of order unity, and χ is $\overline{\nu_p(\nu_p - 1)}/\bar{\nu}^2$, where ν_p and ν are the prompt and total number of neutrons per fission, respectively.

In the prompt neutron approximation at time lags shorter than the time constant of the shortest lived delayed neutron group, the delayed neutron contribution can be ignored so that

$$s_o = \frac{\beta - \rho}{\Lambda} \; , \; A_o = 1/\Lambda \quad ,$$

$$G(s_o) = \frac{0.5}{(\beta - \rho)} \quad ,$$

where β is the effective delayed neutron fraction, Λ is the prompt neutron generation time, and ρ is the reactivity.

Hence in the prompt neutron approximation, the correlation functions have the form

$$R_{11}(\tau) = X\,\delta(\tau) + Y \exp(-\alpha|\tau|) \quad , \tag{5}$$

$$R_{12}(\tau) = Z \exp(-\alpha|\tau|) \quad , \tag{6}$$

$$\alpha = (\beta - \rho) / \Lambda \quad , \tag{7}$$

where α is the prompt neutron decay constant and X,Y,Z are constants.

The zero time lag peak of the auto-correlation (first term in Equation (5)) is due to the detector shot noise and is not present in the cross-correlation function. The amplitudes of the exponential terms contain information on the reactor system but, unfortunately, this information could not be used because of the difficulties in determining the absolute detector efficiency in the reactor.

The above formulae derived for a point reactor model are valid only for the fundamental mode neutron distribution. Except for weakly coupled

systems, reactors at or near critical have the harmonic modes well separated from the fundamental. At increasing subcriticality, however, the harmonic modes become more significant and the above theory requires modification.

The power spectrum of the neutron fluctuations is obtained by Fourier transformation of Equations (5) and (6), giving the auto-power spectral density

$$S_{11}(\omega) = X' + Y' \frac{\alpha}{\alpha^2 + \omega^2} \quad , \tag{8}$$

and the cross-power spectrum

$$S_{12}(\omega) = Z' \frac{\alpha}{\alpha^2 + \omega^2} \quad . \tag{9}$$

3. EXPERIMENTAL PROCEDURE

The neutrons were detected by two large BF_3 proportional counters (diameter 50 mm, active length 40 cm, type 40EB70/50/G; 20th Century Electronics Ltd) with nominal efficiencies of 73 counts s^{-1} (unit thermal neutron flux)$^{-1}$. The data acquisition system (Figure 1) recorded data from each detector separately. Pulse detectors were used to avoid 50 Hz interference and their high efficiency provided a good signal-to-noise ratio.

The detector pulses were amplified and discriminated to give uniform amplitude pulses for all detector pulses exceeding the discriminator bias. The output pulses were then integrated by a diode pump countrate circuit to produce an analogue signal whose amplitude was proportional to the pulse repetition frequency. The storage capacitor network of the ratemeter was essentially a low-pass filter having a double RC frequency response function with an attenuation of 2.2 dB at 1.0 kHz.

The countrate circuit output was recorded on an AMPEX magnetic tape recorder (model FR-1300) for off-line analysis. Two frequency modulated channels having a flat frequency response up to 1.25 kHz were used to record the noise signals. Experimental investigations determined that the upper frequency cutoff of the tape recorder was the limiting factor in the high frequency content of the recorded data.

The data analysis system is shown in Figure 1. A tape speedup factor of eight was used on playback but, in the following discussion, all references to time will be to real or record time and not playback time.

The signals from the tape recorder were passed through low-pass 16-fold RC filters (Rockland model) which provided attenuation of 3 dB at 105 Hz and 48 dB at 500 Hz. The RC filters were used in preference to the Butterworth filters to avoid oscillation on the zero lag peak of the auto-correlation function.

After filtering, the auto-correlation function for each signal and the cross-correlation function were determined using a Hewlett-Packard correlator (Model 3721A). The signal was sampled every 2.664 milliseconds and a maximum of 128K samples could be accumulated per correlogram. Thus, approximately 350 seconds of recorded data were sampled for each correlogram. The correlograms were transferred to the AAEC IBM360 computer for detailed analysis.

A calibration signal consisting of a representative pulse repetition frequency ($\sim 10^4$ pulses per second) gated at 100 Hz was fed into the data acquisition system at the discriminator inputs. These calibration signals were used to ensure that the two channels had identical recording characteristics. During analysis, the calibration signals were used to compare the two channels for discrepancies in phase or amplitude; no significant errors were observed. Also, correlograms of the calibration signals provided information on the timing characteristics of the system - when the mean sampling rate for the correlogram was 2.664 milliseconds, the maximum deviation from the mean was measured to be 0.004 milliseconds.

To estimate the pickup from one channel to the other, the calibration signal was input to one channel only; a pickup of 0.12 per cent on the other channel was measured with a possible upper limit of 0.24 per cent. The error in the data analysis due to the pickup effect was considered to be negligible.

Since the record and analysis instrumentation condition the original reactor noise signal, it is important to demonstrate that no essential information was lost during any of the conditioning processes. The three components which dominate the conditioning processes are the countrate circuit, the tape recorder and the analysing filter. Using a combination of calculation, calibration and manufacturers' specifications, the overall system frequency response function was obtained (Figure 2) and shown to be dominated by the analysing filter frequency response. Superimposed on Figure 2 are the theoretical reactor-power spectra (Equation 7) for prompt neutron decay constants of 25 and 50. Clearly from this figure, the reactor noise information is within the limits of the conditioning equipment

frequency bandwidth. The effect of the frequency response on the correlogram is to convolve the ideal correlogram with a window function that is the Fourier transform of the frequency response. Such a convolution does not change the exponent of a single exponential type correlogram provided data at short time lags is excluded.

4. THE MOATA REACTOR AND THE CRITICAL ASSEMBLIES

The AAEC Moata reactor (a UTR-10 type system) is a light-water moderated and cooled, heterogeneous thermal reactor. The characteristic features of the design of the UTR system are evident in the schematic diagram (Figure 3): two enriched ^{235}U fuel regions or cores are separated by a 457 mm graphite coupling region and surrounded by a graphite reflector. Each core behaves as a semi-independent subcritical system relying on the exchange of neutrons (primarily thermal) between the cores to sustain the critical operation of the reactor as a total system. Seemingly, the coupled core geometry could lead to a wide spatial variation in reactor parameters.

Relevant geometric parameters for the Moata reactor are shown in Table 1(a) and the corresponding values for the mockup assemblies are included for comparison. The hydrogen to ^{235}U (H/U) atom ratio is an average value for the core and indicates a well-moderated system. Table 1(b) contains the dimensions of graphite blocks located on the four faces of the Moata core (Figure 4). These graphite blocks, designed for experimental access, have a significant effect on the neutron generation time.

The operation of the Moata reactor at very low power (milliwatts) for several hours was difficult owing to changes in water temperature, *etc.* Further, following sustained operation at 100 kilowatts, the gamma background from decay of accumulated fission products was so high that neutron pulses could not readily be extracted from the detector output signal. These two facts limited the number of experiments carried out on Moata. The construction of Moata restricted the possible number of experimental access locations adjacent to the fuel slabs - indeed, only two locations, ER-5 and ER-6, proved to be convenient. Consequently, spatial dependence could not be determined for Moata.

A series of four Moata mockup assemblies were constructed on the critical facility. The ^{235}U to hydrogen atom ratios of these assemblies and the Moata reactor were approximately the same, but the light

TABLE 1(a)

PHYSICAL PARAMETERS FOR THE MOATA REACTOR AND THE MOCKUP ASSEMBLIES

	Moata	Mockup Assemblies
Critical Mass kg ^{235}U	3.016	M1 2.850 M2 2.983 M3 2.894 M4 2.612
$H/^{235}U$ Ratio	630:1*	500:1*
Fuel/Moderator Slab		
thickness (mm)	148.4	100
width (mm)	519.1	500
height (mm)	584.2	610

*Note: Two-dimensional average values for the fuel-polythene region only; does not include the top and bottom reflectors.

TABLE 1(b)

DIMENSIONS OF GRAPHITE FILLED EXPERIMENTAL CAVITIES IN THE MOATA REACTOR

Location	Height (mm)	Width (mm)	Length (mm)
East face (thermal column)	1219	1524	1524
West face	762	762	2883
North face	610	610	915
South face	610	610	915

water coolant/moderator was replaced with polythene sheets in the zero-power assemblies. Each fuel slab in the mockup assemblies consisted of six aluminium boxes containing the strips of fuel and polythene; two different sized boxes were used with the fuel density lower in the larger boxes (1A, 2A, 1D and 2D). Although the essential geometric features of Moata were retained, the individual mockup fuel slabs were 100 mm thick compared to Moata slab thickness of 148.4 mm. The coupling region and the reflector were constructed of graphite blocks (dimensions 100 mm x 100 mm x 800 mm) and this gave an almost unlimited number of detector positions.

TABLE 2

CRITICAL FACILITY ASSEMBLIES

Assembly	Core Separation (mm)	Fuel Configuration	Coupling Region	
			Material	Atom Number Density $_{cm^{-3}}$ x 10^{-20}
M1	450	A	Graphite	C:850
M2	600	A	Graphite	C:850
M3	800	B	Graphite	C:850
M4(a)	450	B	Graphite + Cd/Pb	C:850
				Pb:0.04
				Cd:0.001
M4(b)	450	B	Graphite + Polythene	C:853
				H:6.6
M4(c)	450	B	Graphite	C:850
M4(d)	450	B	Graphite + Iron	C:850
				Fe:7.0

Note: Fuel Configuration
A - lower fuel density boxes closest to assembly centre line.
B - higher fuel density boxes closest to assembly centre line.

The first assembly constructed(M1, Figure 5) most closely approximated the Moata geometry. The most significant change between assemblies M1, M2 and M3 was the increasing separation between the fuel slabs (Table 2). A secondary change was the rearrangement of the fuel so that the higher fuel density boxes were toward the assembly centre line for assemblies M3 and M4.

Mockup M4 reverted to the same slab separation as M1 and was used, primarily, to investigate the effect of the coupling region properties on the prompt neutron generation time. These properties were varied by placing slabs of poisoning material ($(C_2H_2)_n$, Cd/Pb,Fe) in a machined slot in each graphite block of the coupling region.

5. EXPERIMENTAL RESULTS

5.1 Exponential Least-squares Fit

The correlograms (Figures 6 and 7) clearly show that the correlation functions depart from a simple exponential near the zero time lag. The auto-correlation function contains a large zero lag spike due to a random component in the recorded signal; this spike was widened by the window function of the analysing filter. The cross-correlation function is

modified by the effects of the coupling between the two cores, and by neutron transport time effects. The short time lag data have been analysed by Harries [1976] on the basis of a two-node reactor model. To avoid the complication of the short time lag phenomena in the present analysis, the first five data points were neglected in the determination of α.

Using a least-squares fitting program, each correlogram was fitted by a function of the form

$$F(t) = A_1 \exp (A_2|t|) + A_3 \quad , \tag{10}$$

where A_1, A_2 and A_3 are the the three fitted parameters. The convergence criterion for the fitting procedure was a variation of less than 0.001 per cent in all three parameters between successive iterations.

For each 350 seconds of data, the two auto-correlograms (R_{11}, R_{22}) and the two cross-correlograms (R_{12}, R_{21}) were determined and individually analysed to determine a value of A_2. The four estimates of A_2 were averaged to decrease random counting and fitting errors. However, the estimates were not completely independent because background prompt neutron chains tended to affect all correlograms equally. An estimate of the reproducibility could only be obtained by determining the mean A_2 over successive time intervals. At least four time intervals were used for each experiment which enabled a standard deviation to be determined.

Several 400-point correlograms were constructed using the 'Delay Offset' facility of the correlator to test the fit to the background. The inclusion of the extra 0.75 seconds of data in the least-squares fit changed A_2 by less than ± 0.5 per cent.

5.2 Reactivity and Delayed Neutron Corrections

The prompt neutron generation time at critical is determined from the experimental values of A_2 by correcting for the effects of delayed neutrons correlated to the initiating prompt chain, and for the effects of the system reactivity.

The single exponential correlation function used in the data analysis is valid provided the delayed neutron contributions can be neglected. The effect of this approximation had to be evaluated because the maximum time lag used in this experiment (0.2664 s) was comparable to the decay period of the shortest lived delayed neutron group.

The theoretical correlation function, including delayed neutrons (Equations (3) and (4)), was evaluated for different values of α using the

transfer function coefficients and roots given by Keepin [1965]. Utilising the least-squares fitting procedure, a single exponential function (Equation (10)) was fitted to the theoretical correlation function over the same range of lag times as the experimental correlograms. In the limit of large α, where the prompt neutron approximation was valid, the fitted exponent, A_2, was equal to the prompt neutron decay constant, α. The correction for the delayed neutron effect depended on the value of α and the range of lag times over which the fitting procedure was carried out. In consequence, the exponents fitted to the experimental correlograms were corrected by -0.5 per cent for Moata and between -0.24 and +0.13 per cent for the mockup assemblies to give the experimental values of α.

The very low reactor power used to avoid excessive detector countrates, and the background neutron source meant that the reactor assembly was significantly subcritical during the experiments. The reactivity was determined from the position of the calibrated control rods as a function of reactor power. The values of α quoted are the critical values calculated from the measured α and the reactivity.

5.3 Deadtime, Perturbation and Spatial Effects

Amplification and shaping of the detector pulses by the main amplifier introduced a deadtime of 2 microseconds into the data acquisition system. Further, the ratemeter response function was non-linear at countrates near 10^5 pulses per second owing to a pulse pileup effect. An estimate of these 'deadtime' effects on the measurement of α was obtained by carrying out experiments at two different reactor power levels, chosen so that there was a factor of two difference in the channel countrate. As exemplified by Table 3, the results suggest no systematic dependence on countrate over the range used in the experiments.

To assess the effect of the perturbation on the measurement of α with the detectors located in the graphite reflector, the large 50 mm diameter detectors were replaced with two pairs of 25 mm diameter detectors (type 12EB40) for two experiments. Because of the loss of efficiency, the data had larger errors, but the results suggested that α was unchanged.

Although the mockup assemblies provided an opportunity to study spatial effects, the range of detector positions that could be utilised was limited by the conflicting requirements of high efficiency and low perturbation to the assembly. Experiments were only carried out for detector reactivity perturbations of less than 0.004 $\Delta k/k$ - the amount

TABLE 3

TEST FOR SYSTEMATIC COUNTRATE EFFECTS

Mockup Assembly	Experiment	Reactor Power (mW)	Reactivity x 10^5 ($\Delta k/k$)	Detector Position	Countrate x 10^{-4} (s^{-1})		α_c (s^{-1})
					Channel A	Channel B	
M1	1	0.68	8.0	C-C	8.0	7.2	26.0±0.2
	3	0.30	18.0	C-C	4.0	3.5	25.4±0.8
	2	0.30	18.0	B-B	5.1	5.0	25.0±0.2
	4	0.15	37.0	B-B	2.2	2.1	24.0±0.6
M2	1	0.30	11.0	A-A	4.0	4.0	24.0±0.2
	2	0.14	24.0	A-A	2.8	2.7	24.7±0.9
M3	1	0.18	20.0	A-A	2.4	2.7	28.5±1.1
	2	0.08	41.0	A-A	1.3	1.4	29.0±0.7

Note: Each experiment had at least four sequential estimates of α. The error attached to the mean experimental value of the prompt neutron decay constant, α_c, is the standard deviation of the mean from four estimates.

which could be compensated for by control rod movements. Up to this reactivity perturbation, absorption of neutrons by either the control rod or the detector should be of no consequence to the neutron generation time. If more fuel had been added to increase the excess reactivity available, the neutron generation time would probably have changed because of the additional fuel. The very small detectors (6 mm diameter BF_3 type 5EB70/6), which could have been positioned in the fuel regions without causing too high a reactivity perturbation, had efficiencies that were too low to give meaningful results, since the amplitude of the correlated component of the correlation function is proportional to the square of the detector efficiency in counts per fission (Equation (3)).

A representative sample of the spatial effect results for the three mockup assemblies (M1, M2, M3) is given in Table 4. Within the uncertainties attached to the experimental values, the measurement of α_c is independent of the detector positions. These results agree with the results of Dragt [1968] who measured the auto-correlation function with detectors set well into a reflector and thermal column, and found no change in the value of α_c.

The best estimate of α_c for each assembly was obtained from the mean

TABLE 4

SPATIAL DEPENDENCE ON THE PROMPT NEUTRON DECAY CONSTANT, α_c

Mockup Assembly	Experiment	Reactor Power (mW)	Reactivity x 10^5 ($\Delta k/k$)	Detector Positions	α_c (s^{-1})
M1	2	0.30	18.0	B-B	25.0 ± 0.2
	3	0.30	18.0	C-C	25.4 ± 0.8
M2	1	0.30	11.0	A-A	24.0 ± 0.2
	3	0.23	15.0	A-B	24.3 ± 0.8
M3	1	0.18	20.0	A-A	28.5 ± 1.1
	2	0.30	11.0	C-C	29.2 ± 0.7
	3	0.22	13.0	A-A	30.2 ± 1.1
	4	0.26	10.0	B-B	29.0 ± 0.9
	5	0.22	13.0	B-B	29.0 ± 0.4

Note: Detector Position A - distance between the detector centre line and the core mid-plane was 200 mm.

Detector Position B - 300 mm distant.

Detector Position C - 400 mm distant.

Detectors on opposite sides of assembly except for M2, experiment 3.

TABLE 5

EXPERIMENTALLY DETERMINED PROMPT NEUTRON DECAY CONSTANT, α_c AND THE DERIVED NEUTRON GENERATION TIME, Λ

Reactor Assembly	α_c (s^{-1})	Λ (μs)
Moata	44.8 ± 1.3	165
M1	24.9 ± 0.4	297
M2	24.4 ± 0.3	303
M3	28.9 ± 0.3	256
M4(a)	31.8 ± 0.4	233
M4(b)	29.1 ± 0.5	254
M4(c)	30.8 ± 0.6	240
M4(d)	35.8 ± 0.6	207

Generation time derived assuming $\beta_{eff} = 0.0074$.

of all measurements on that particular assembly. The results are shown in Table 5 - the errors are the standard deviation in the mean α_c data.

6. THEORETICAL CALCULATION OF THE PROMPT NEUTRON DECAY CONSTANT

The prompt neutron generation time and the effective delayed neutron fraction have been calculated for the Moata reactor and the mockup assemblies using the computer codes POW and DXYZ. POW [Pollard 1974] is a general purpose, two-dimensional (2D) neutron diffusion and kinetics code which uses buckling terms to account for neutron leakage in the unspecified direction. DXYZ [Doherty 1974(a)] is a multigroup, finite difference diffusion code for three-dimensional (3D) geometry. Both codes are segments of the AUS modular scheme for reactor neutronics computations [Robinson 1976]. The calculations were carried out with four energy groups, the group cross sections being derived from 128 group libraries based on ENDF/B data by modules of the AUS scheme.

Sufficient geometric symmetry was imposed for a quarter core calculation with the 2D code and a one eighth core calculation with the 3D code. This was necessary to limit computer (CPU) time, but it did introduce uncertainties because of the asymmetries in the fuel loading, the top and bottom reflectors, the experimental cavities in Moata, and the effects of small holes for control rods, neutron detectors, sources *etc.*

The prompt neutron generation time, Λ, was calculated from the change in the multiplication constant due to a uniform spatial distribution of (1/v) absorber. Four-group (1/v) cross sections were condensed from 43-group data in the cell calculation using adjoint weighting. The 2D code then calculated Λ by the standard perturbation formalism. For the 3D code, which has no adjoint flux calculation, Λ was derived from the difference between two 'k' calculations. The delayed neutron fractions, β_i, were taken from Tomlinson [1972], and the spectrum weighting functions, γ_i, were calculated for each delayed group by the 2D code.

In the 2D representation, the calculated prompt neutron generation time was sensitive to the assumed buckling in the unspecified direction. The fuel-polythene region had a total height of ~700 mm and the graphite reflector and coupling region had a height of ~1400 mm. As a result, in M1 for example, the experimentally determined (foil scan) thermal flux distribution gave a buckling of 12.9×10^{-4} cm^{-2} (height 875 mm) in the fuel-polythene region, and 6.3×10^{-4} cm^{-2} (height 1250 mm) in the graphite regions close to the fuel. When these two group-independent bucklings

were used in the 2D calculation, the predicted prompt neutron decay constant, α_c, was in reasonable agreement with the measured value but the calculated multiplication constant, k_{eff}, was ~7 per cent too high. A reasonable result for k_{eff} could only be obtained if the fuel buckling of 12.9×10^{-4} cm^{-2} was used for all mesh points, but α_c was then ~40 per cent too high. This is attributed to the incorrect weighting of the neutron lifetime in the reflector.

The results of the calculations are shown in Table 6. Because of the difficulty in defining a unique buckling to allow for the complex leakage effects in the unspecified direction, the agreement between experiment and the 2D calculation was somewhat contrived. The same mesh intervals and material cross sections were used in the 3D calculations as in the 2D calculations. The better geometric representation of the 3D calculation gave values of k_{eff} and α_c that are in better agreement with the experimental results without the somewhat arbitrary assignment of bucklings necessitated by attempted two-dimensional representations.

The calculated flux distributions for Moata, mockup M1, and mockup M3 are shown in Figures 8, 9 and 10 respectively. The flux ratios between the centre of the coupling region and the centre of the fuel region are in reasonable agreement with experiment. However, difficulties in modelling the edges of the fuel boxes have caused significant errors in the calculated fluxes near the interface between the fuel region and the graphite.

7. DISCUSSION

Perhaps the most noteworthy feature of the results is the difference in α_c between Moata and the mockup M1, despite their similar characteristics of critical mass, fuel-to-moderator atom ratio and macroscopic geometry.

The reason for the difference is evident from a comparison of the thermal flux profiles of Moata (Figure 8), mockup M1 (Figure 9) and mockup M3 (Figure 10). These indicate that the core region thermal flux is considerably more depressed in the mockup assemblies than in Moata. This was due to the thinner core slabs of the mockup assemblies allowing greater neutron leakage to the reflector leading, in turn, to the observed longer neutron generation time.

Assemblies M1 and M4(c) had the same core separation, but different fuel arrangements. In the M1 assembly, the lower fuel density boxes were toward the centre line of the assembly, whereas for M4(c) the

TABLE 6

POW (2D) AND DXYZ (3D) CALCULATIONS OF THE PROMPT NEUTRON DECAY CONSTANT, α_c

Mockup Assembly	Code	Bucklings x 10^4 cm^{-2}		Calculation				Experimental $\alpha_c s^{-1}$
		Fuel Region	Graphite Region	k_{eff}	β_{eff} x 10^3	Λ μs	$\alpha_c s^{-1}$	
M1	2D	12.9	12.9	1.023	7.314	169.0	43.3	
		12.9	6.3	1.068	7.219	240.2	30.0	24.9 ± 0.4
	3D	-	-	1.032	7.219	255.4	28.3	
M2	2D	12.9	6.3	1.051	7.248	249.8	29.0	24.4 ± 0.3
	3D	-	-	1.016	7.248	263.8	27.5	
M3	2D	12.9	6.3	1.043	7.281	224.2	32.5	28.9 ± 0.3
	3D	-	-	1.011	7.281	236.3	30.8	
M4(c)	2D	12.9	6.3	1.072	7.225	229.5	31.5	30.8 ± 0.6
	3D	-	-	1.037	7.225	239.0	30.2	
Moata	2D	12.9	12.9	1.026	7.252	164.0	44.2	44.8 ± 1.3

higher fuel density boxes were toward the centre. This caused α_c to change from 24.9 ± 0.4 s^{-1} for assembly M1 to 30.8 ± 0.6 s^{-1} for M4(c). The experimental thermal flux profiles of the M4(c) assembly suggested a greater flux peaking in the central fuel region (in the higher fuel density boxes). This flux peaking would cause a lower proportion of neutrons in the graphite and hence the shorter generation time.

A smaller change in measured α_c occurred with increasing core separation. Comparison of the M1 and M2 results shows a general decrease in α_c with increasing core separation, due mainly to the increase in volume of graphite in the coupling region. A similar trend is evident in the M4(c) and M3 results.

The graphite absorption cross section is so low that leakage is the principal means of neutron loss from the reflector. The lifetime of neutrons in different regions of Assembly M1 was estimated from the 2D diffusion calculation and leakage considerations. The mean adjoint-flux weighted lifetime for the fuel moderator is approximately 56 μs compared with a leakage dominated lifetime of about 1700 μs for the graphite reflector. The net generation time for the assembly was 297 μs.

These lifetimes can be used in a one-group reflected core model [Karam 1964] to show that the bare core reactivity is about -0.15 Δk/k This implies that about 86 per cent of the fission-causing neutrons do not enter the graphite reflector.

8. COMPARISON WITH OTHER REACTORS

There have been a number of experiments on graphite reactors of the UTR type with two fixed planar fuel slabs and a graphite coupling region. The Argonaut reactors, when loaded with two 'annular' slabs, show remarkable similarity to the UTR type. However, the detailed differences between reactors can lead to large discrepancies in measured α. The results of published measurements of α in UTR and Argonaut reactors are given in Table 7.

MOATA

Marks [1968] used a reactivity oscillator, with digital correlation techniques for improvement of signal-to-noise ratio at high frequency, to determine the zero-power transfer function of Moata. The reactivity oscillator was located at the geometric centre of the coupling region and the ion chamber detector in experimental access location ER-5. The high frequency break-point of the transfer function was estimated to be ω_H = 9.24 Hz which implied a value of α = 51.8 s^{-1}. Marks assumed

TABLE 7

EXPERIMENTAL DETERMINATIONS OF THE PROMPT NEUTRON DECAY CONSTANT, α_c, AND PROMPT NEUTRON GENERATION TIME, Λ, FOR UTR AND ARGONAUT REACTORS

Reactor	Slab Separation	Critical Mass kg ^{235}U	α s^{-1}	Λ μs	Reference
Moata	457 mm	3.016 (90% enriched)	44.8 ± 1.3	165	This report
			51.8	124	Marks [1968]
UTR (London)	457 mm	2.95 (90% enriched)	64.0 ± 4.0		Leonidou & Mansfield [1971]
URR	305 mm	3.3 (90% enriched)	30.5 ± 2.0	246 ± 16	Jeffers & Corpus [1968]
			28.5, 29.9		Humphreys & Jeffers [1970]
			27.0		Jeffers [1970]
			33.5 ± 0.6	(221)	McDonnell & Harris [1972]
UFTR	305 mm	3.5 (20% enriched)		280*	Uhrig [1964]
Argonaut (Argonne National Laboratories)	610 mm dia.	3.4 (20% enriched)	45.3 ± 6.3	154 ± 21	Cohn [1959]
				160	Wilson [1961]
				180 ± 5*	Pawlicki [1961]
Argonaut (Karlsruhe)	610 mm dia.	5.541 (19.8% enriched)	36.7 ± 1.3		Seifritz & Albrecht [1968]
Argonaut (Petten)	610 mm dia.	3.645 (90% enriched)	50.7 ± 0.8*	145.6 ± 6	Dragt [1968]
			44.4 ± 0.8	166	

Note: (1) Asterisk denotes the result is from experiments carried out on a one-slab loading of the reactor.

(2) Brackets in column 5 indicate that the value was not published explicitly, but rather inferred from the experimental data.

a value of 0.0064 for β and calculated a generation time, Λ, of 124 μs. However, more recent calculations give a value of 0.0074 for β which would give 143 μs for Λ.

UTR-100, LONDON

The UTR-100 at the University of London is almost identical to Moata. Leonidou & Mansfield [1971] were primarily concerned with the evaluation of the coupling coefficient of the UTR-100. Using a pulsed neutron source technique and a method of analysis based on a simplified version of the kinetic equations [Baldwin 1959], an estimate of α at delayed critical was inferred from results measured at various levels of subcritical reactivity. The value of α quoted was $64 \pm 4\ s^{-1}$.

URR, RISLEY

The University Research Reactor (URR) at Risley is a similar reactor to Moata (two slabs of 90% enriched ^{235}U - critical mass 3.3 kg), but with a 300 mm coupling region [Bridge *et al.* 1965]. Jeffers & Corpus [1968] used a reactivity oscillator centrally located in the coupling region and, assuming a β of 0.0075, the experimental data was fitted by the zero power transfer function. The result was reported as a prompt neutron generation time of 246 ± 16 μs.

Humphreys & Jeffers [1970] determined α from an investigation of the inherent noise in the URR. The cross power spectral density (CPSD) function of two detectors positioned immediately adjacent to each other in an experimental access location near one core gave the value of α as $28.5\ s^{-1}$. The CPSD function for two symmetric detector locations gave an α of $29.9\ s^{-1}$. It is difficult to comment on the relevance of the difference between these two values since an error analysis was not included.

The spatial transfer function of the URR was calculated using two-group diffusion theory [Jeffers 1970]. Using a one-dimensional model, the transfer function was calculated by introducing an oscillating thermal neutron absorber outside one core and calculating the magnitude and phase of the resultant thermal flux oscillations at the reactor centre line. These theoretical Bode plots had a break frequency of 4.3 Hz implying a value for α of $27.0\ s^{-1}$.

McDonnell & Harris [1972] employing a pulsed neutron source technique to determine subcritical reactivities, evaluated the delayed critical prompt neutron decay constant for the URR to be $33.5 \pm 0.6\ s^{-1}$,

the average of a number of experiments. Theoretical models were analysed to enable a comparison between measured values of α with estimates calculated from an appropriate set of cross section data and a multi-group diffusion code. The 'poison removal' technique [Kear & Riederman 1962] was used to calculate values of α at various levels of reactor subcritical reactivity. The delayed critical α was calculated to be 37.5 s^{-1} in reasonable agreement with experiment. However, considerable difficulty was encountered in calculating α at large subcritical reactivity because of the difficulty in calculating prompt and delayed flux distribution.

The published information on the measurement and calculation of the prompt neutron decay constant on the URR is comprehensive. The consistency between the results of different experimental techniques is a notable feature.

UFTR

The University of Florida Training Reactor (UFTR) is similar to the URR. Uhrig [1964] performed a pulsed neutron source experiment in a one-slab loading of the UFTR, where the neutron source was located on the reflector side of the core and the ion chamber detector in the centre of the coupling region. Again, the information on α was deduced from the break frequency of the power spectral density function and the result was published as the effective neutron lifetime of 280 μs for the reactor. This would give an α of 26.4 s^{-1} for β_{eff} equal to 0.0074.

A random reactivity input device and two ion chamber detectors symmetrically located approximately 450 mm into the graphite reflector were used by Boynton & Uhrig [1964] to determine the reactivity of UFTR from the reactor transfer function. If a prompt neutron lifetime of 280 μS was assumed, then acceptable agreement was achieved in determining the reactivity of each core.

ARGONAUT (ANL)

The Argonaut low power research reactor at Argonne National Laboratories (ANL), when loaded in a two-slab geometry, has similar characteristics to the UTR systems. Cohn [1959] used the frequency spectrum of the reactor noise to determine a value of 45.3 ± 6.3 s^{-1} for α. The relatively large error in α was attributed to the limited band width of the experimental equipment. Assuming an effective delayed neutron function β of 0.007, a generation time of 154 ± 21 μs was obtained.

For one-slab loading of the ANL Argonaut, Pawlicki [1961] determined a value of neutron generation time of 180 ± 5 μs from the experimental transfer function. Wilson [1961] also determined the reactor transfer function from reactivity oscillator experiments. A plot of the transfer function gain was constructed and compared to the theoretical transfer function of a reactor with a neutron lifetime of 160 μs.

ARGONAUT (KARLSRUHE)

Seifritz & Albrecht [1968] performed experiments in the Argonaut reactor at Karlsruhe with both ring core fuel loadings and a two-slab core loading. For the two-slab data which is of interest here, the Karlsruhe Argonaut has a critical mass of 5.541 kg ^{235}U, which is much larger than the other UTRs and Argonauts and suggests a significant difference in the core characteristics. From a frequency analysis of the inherent neutron noise, the auto power spectral density (APSD) and the cross power spectral density (CPSD) functions were obtained. A value of 36.7 ± 1.3 s^{-1} for α was determined from the characteristic break frequency of the PSD functions.

LFR (PETTEN)

The Low Flux Reactor (LFR) at Petten is another Argonaut reactor which has been investigated. With a one-slab loading (1.885 kg ^{235}U) of the LFR, Dragt [1968] analysed the signal from an ion chamber detector located at various distances into the reflector. The reactor noise signal was digitised and a computer accumulated the auto-correlation function. The experimental value of α exhibited no dependence on the location of the detector other than an increase in the error due to a decrease in efficiency as the detector moved further into the reflector. From the information contained in the zero lag peak of the auto-correlation function, and by knowing the absolute fission rate of the reactor, Dragt was able to estimate the value of β_{eff}. Corrections were applied for delayed neutrons and spatial and energy dependence. For the one-slab loading, the prompt neutron generation time was 145.6 ± 6 μs with an effective delayed neutron fraction of 0.738 ± 0.031 per cent. For the two-slab loading (3.645 kg ^{235}U), the prompt neutron decay constant was 44.4 ± 0.8 s^{-1} and, if β_{eff} is unchanged, the generation time would be 166 μs.

9. CONCLUSIONS

The correlation functions of reactor noise have been used to determine the prompt neutron decay constant of the Moata reactor and related mockup

assemblies. The decay constant depended primarily on properties that varied the core-reflector neutron interactions and only secondarily on the core separation.

Two-dimensional diffusion theory calculations of the prompt neutron generation time were in agreement with the experimental value for Moata but up to 20 per cent too low for the mockup assemblies. Three-dimensional calculations removed some of the discrepancy and avoided the necessity of using buckling estimates.

10. ACKNOWLEDGEMENTS

The authors wish to express their appreciation to Mr. J.W. Connolly for many fruitful discussions and for the design and construction of the M1 assembly. We also wish to acknowledge the assistance given by members of the Theoretical Physics Section, particularly Dr. J.P. Pollard and Mr. G.S. Robinson, in the use of the computer codes. The cooperation of the staff of the AAEC Moata reactor and the Critical Facility is also gratefully acknowledged.

11. REFERENCES

Baldwin, G.C. [1959] - Kinetics of a Reactor Composed of Two Loosely Coupled Cores. *Nucl. Sci. Eng.*, 6:320-327.

Boynton, A.R. & Uhrig, R.E. [1964] - Evaluation of Two-region Reactor Parameters by Random Noise Measurements. *Nucl. Sci. Eng.*, 18:220-229.

Bridge, H., Hall, W.B. & Jeffers, D.E. [1965] - The Liverpool and Manchester Universities Research Reactor. *J. Brit. Nucl. Energy Soc.*, 4:85-96.

Cohn, C.E. [1959] - Determination of Reactor Kinetic Parameters by Pile Noise Analysis. *Nucl. Sci. Eng.*, 5:331-335.

Doherty, G. [1974a] - DXYZ - An unpublished report based on ZHEX.

Doherty, G. [1974b] - ZHEX - A Three-dimensional Diffusion Code for Hexagonal Z Geometry. AAEC/E307.

Dragt, J.B. [1968] - Reactor Noise - A Study of Neutronic Fluctuations in Low-power Nuclear Reactors, with Special Emphasis on Accurate Time-Domain Analysis. RCN-101.

Harries, J.R. [1976] - Correlation and Flux Tilt Measurements of Coupled-core Reactor Assemblies.AAEC/E357.

Humphreys, E. & Jeffers, D.E. [1970] - Spatially Dependent Noise Measurements in a Two Zone Reactor. *Atomkernenergie*, 16:132-134.

Jeffers. D.E. [1970] - Spatial Transfer Functions of a Two Core Reactor. *Atomkernenergie*, 16:129-131.

Jeffers, D.E. & Corpus, G. [1968] - Transfer Function Measurements on the Universities' Research Reactor at Risley. *J. Brit. Nucl. Energy Soc.*, 7:146-150.

Karam, R.A. [1964] - Measurement of Rossi-Alpha in Reflected Reactors. *Trans. Am. Nucl. Soc.*, 7:283-284.

Kear, G.H. & Riederman, M.H. [1962] - An Analysis of Methods in Control Rod Theory and Comparison with Experiment. GEAP-3937.

Keepin, G.R. [1965] - Physics of Nuclear Kinetics. Addison-Wesley Publishing Co., Massachusetts.

Leonidou, D.J. & Mansfield, W.K. [1971] - Estimation of the Coupling Coefficient at Various Subcritical Levels of a Symmetrical Two Core Reactor. *J. Inst. Nucl. Eng.*, 12 (Nov/Dec)171-175.

Marks, A.P. [1968] - The Moata Transfer Function. AAEC/TM481.

McDonnell, F.R.N. & Harris, M.J. [1972] - Pulsed-source Experiments in a Reflected Coupled-core Reactor - I. Reactivity Measurements. *Nucl. Energy*, 26:113-128.

Pawlicki, G. [1961] - Neutron Lifetime for the One-slab Loading determined from Transfer Function Measurements. Argonaut Reactor Databook ANL 6285 (W.J. Sturm and D.A. Daavettila, editors), pp 127-128.

Pollard, J.P. [1974] Aus Module POW - A General Purpose 0, 1 and 2D, Multigroup Neutron Diffusion Code including Feedback-free Kinetics. AAEC/E269.

Robinson, G. [1976] - AUS - Australian Modular Scheme for Reactor Neutronics Computations. AAEC/E369.

Seifritz, W. & Albrecht, R.W. [1968] - Measurement and Analysis of the Coupled Core Coherence Function in a Two Node Symmetrical Reactor. *Nukleonik* 11:149-154.

Tomlinson, L. [1972] - Delayed Neutrons from Fission. A Compilation and Evaluation of Experimental Data. AERE-R-6993.

Uhrig, R.E. [1964] - Nuclear Noise Research Program at the University of Florida - Noise Analysis in Nuclear Systems. R.E. Uhrig, Coordinator. TID 7679, pp 251-284.

Wilson, W.E. [1961] - Measurement of the Transfer Function of the Argonaut Reactor. ANL-6410 (W.J. Sturm, editor), pp 286-289.

DATA ACQUISITION :

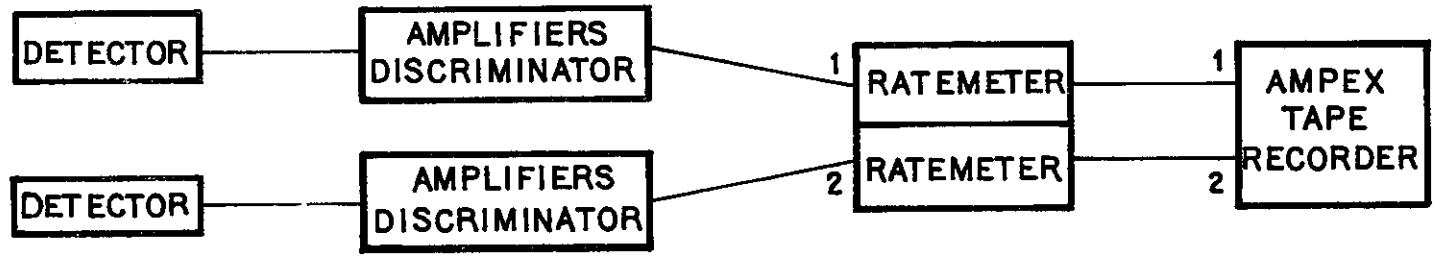

DATA ANALYSIS:

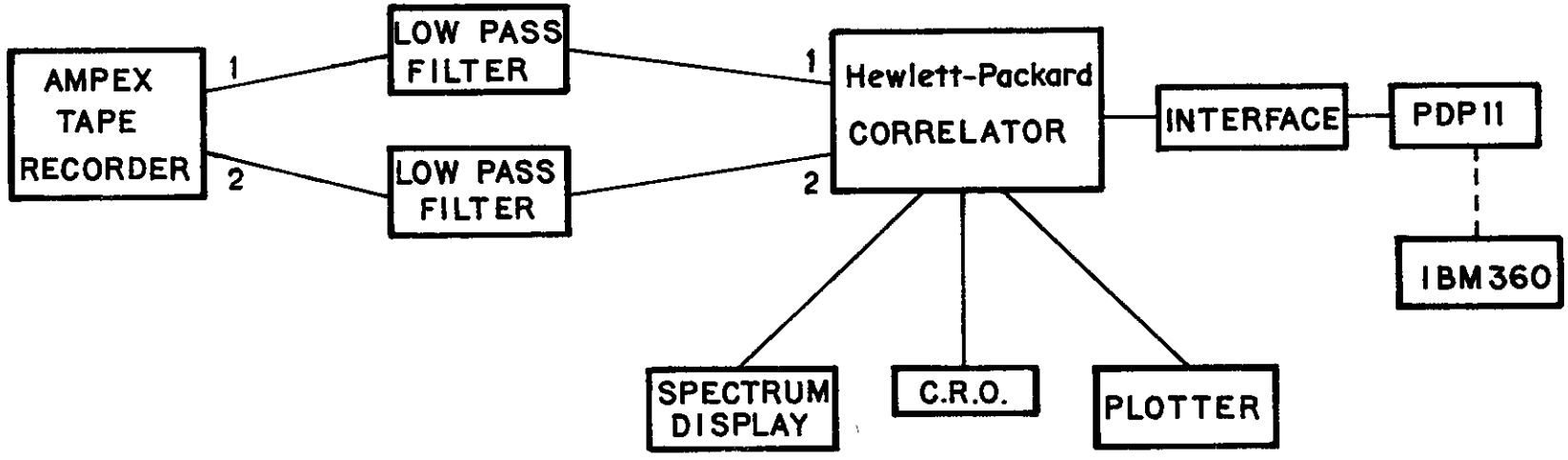

FIGURE 1. SCHEMATIC DIAGRAM OF EXPERIMENTAL EQUIPMENT

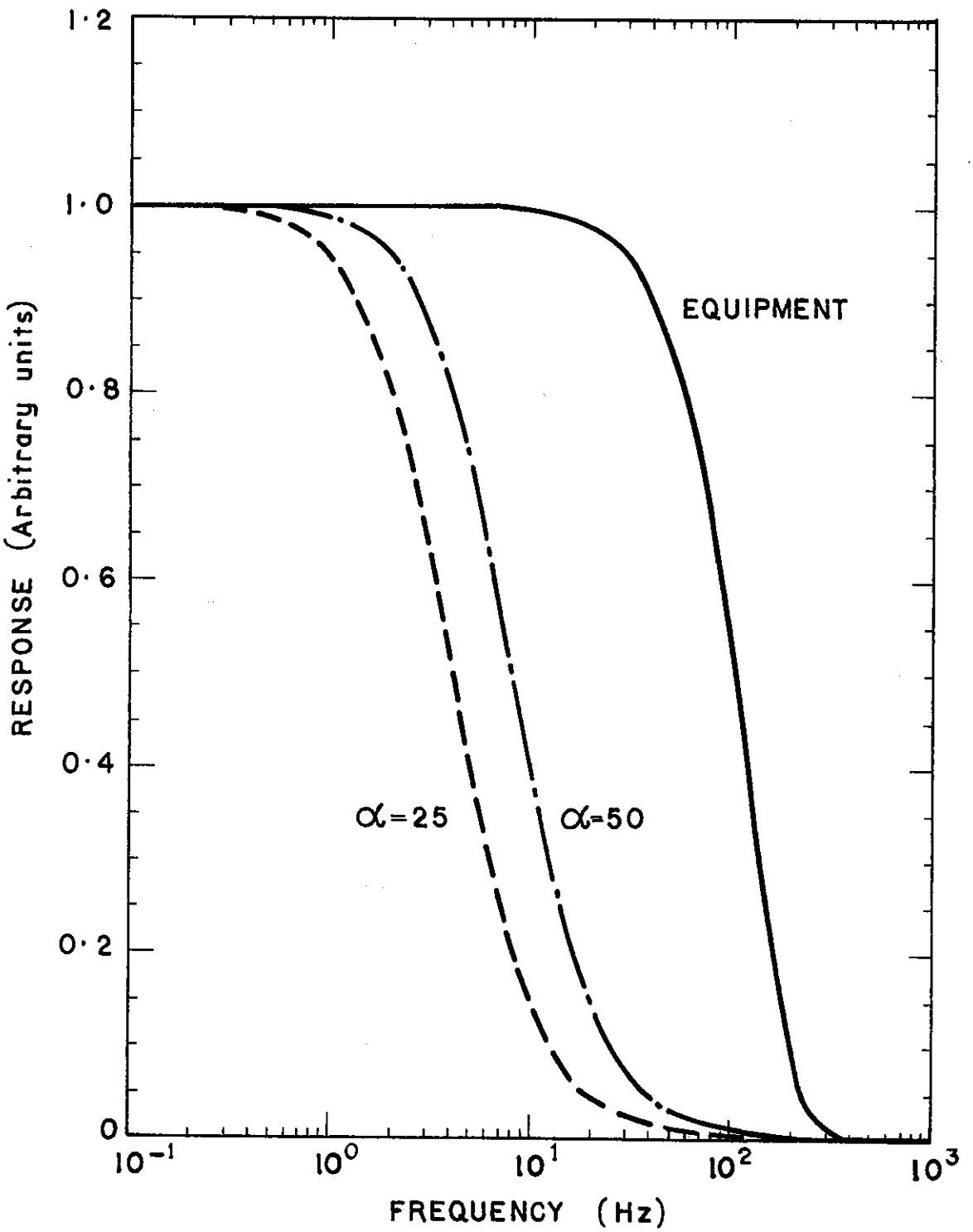

FIGURE 2. FREQUENCY RESPONSE OF EXPERIMENTAL EQUIPMENT AND THEORETICAL REACTOR-POWER SPECTRA

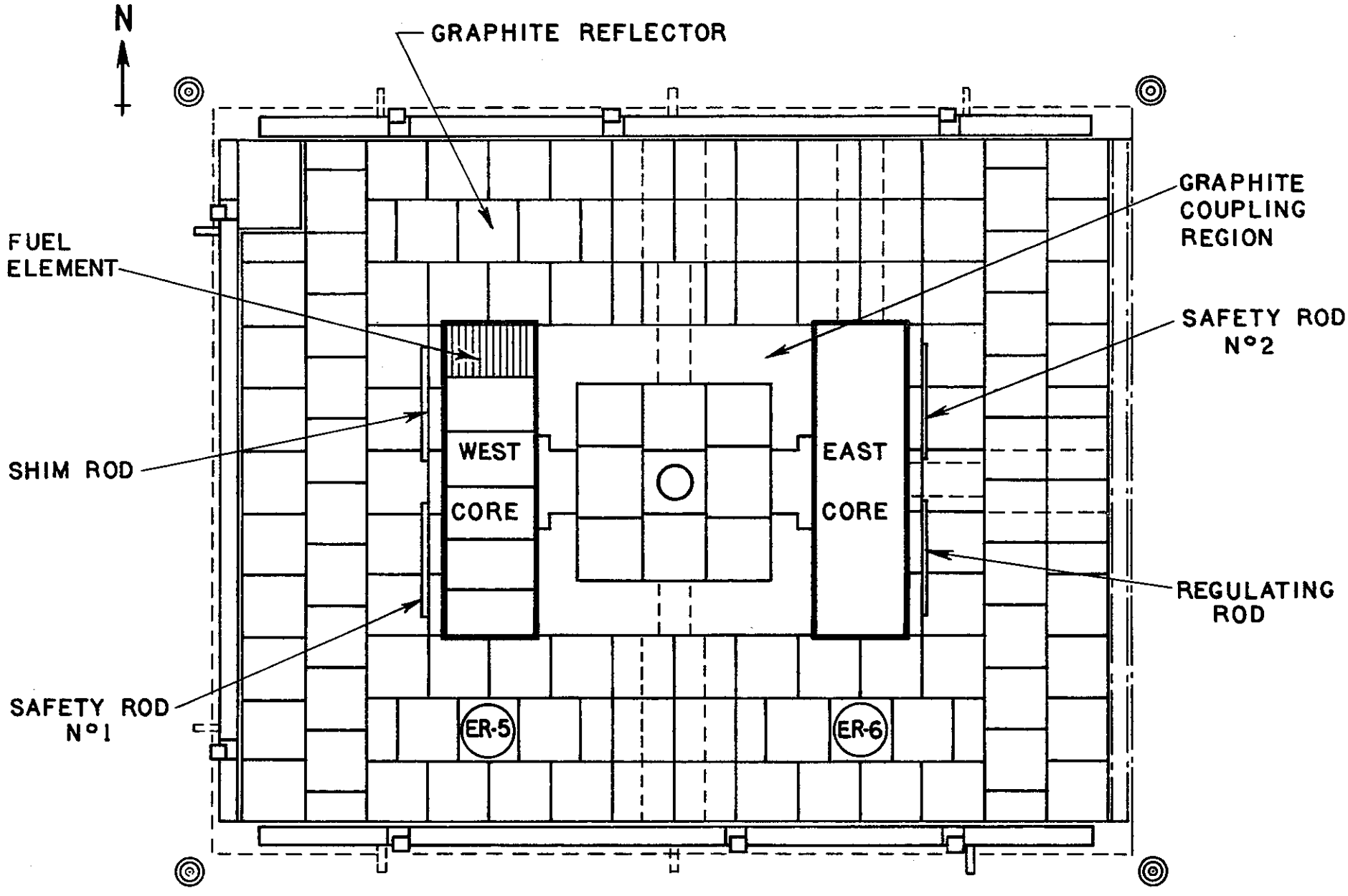

FIGURE 3. MOATA CENTRAL CORE REGION

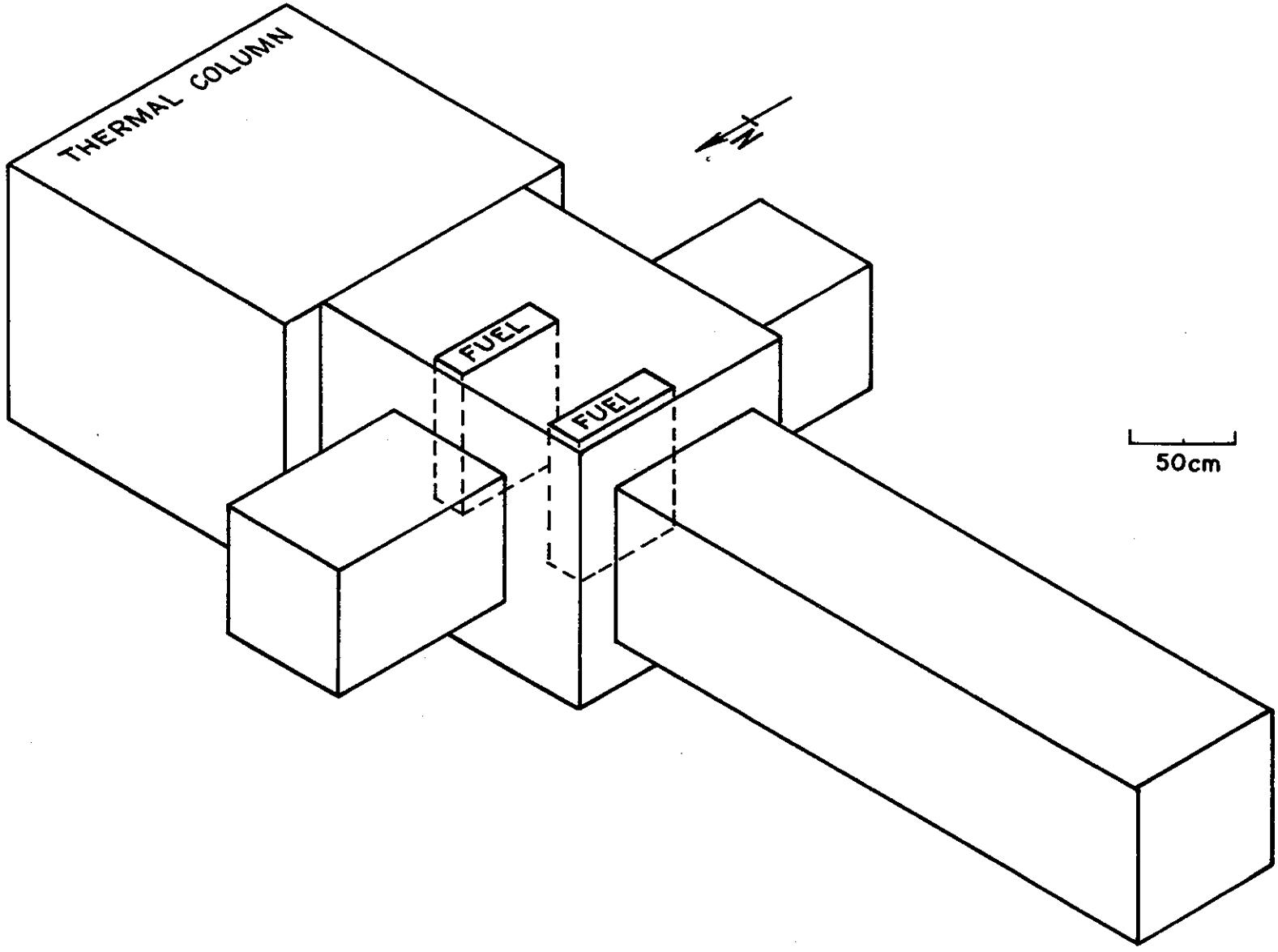

FIGURE 4. SCHEMATIC DIAGRAM OF THE MOATA REACTOR

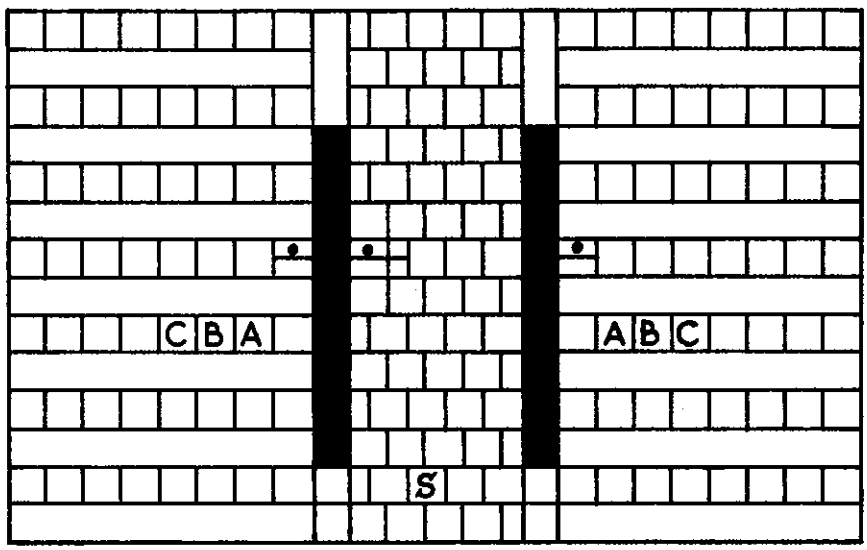

SECTION A-A

S — SOURCE (START UP)
(C) — CONTROL ABSORBER ROD
(S) — SAFETY ROD

SCALE
200mm

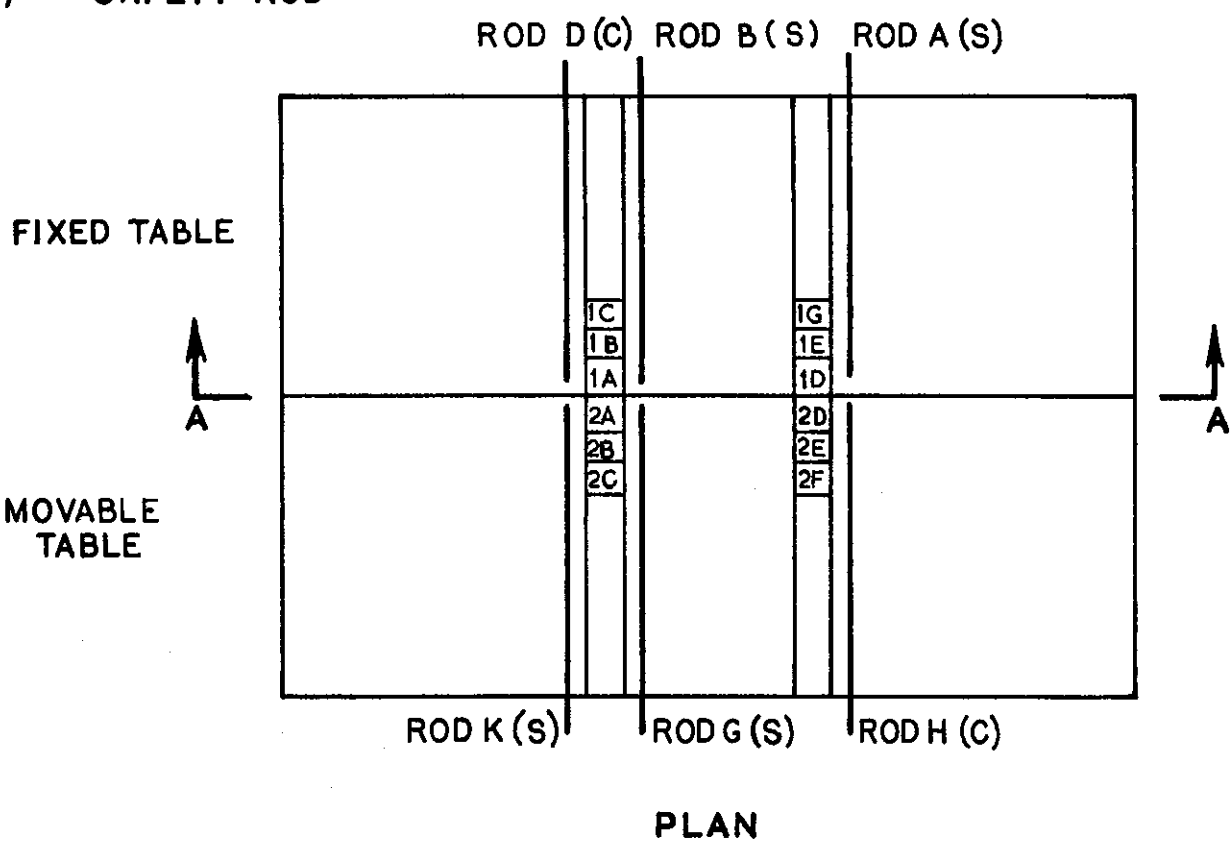

PLAN

FIGURE 5. MOCKUP 1 ASSEMBLY — CORE SEPARATION 450mm

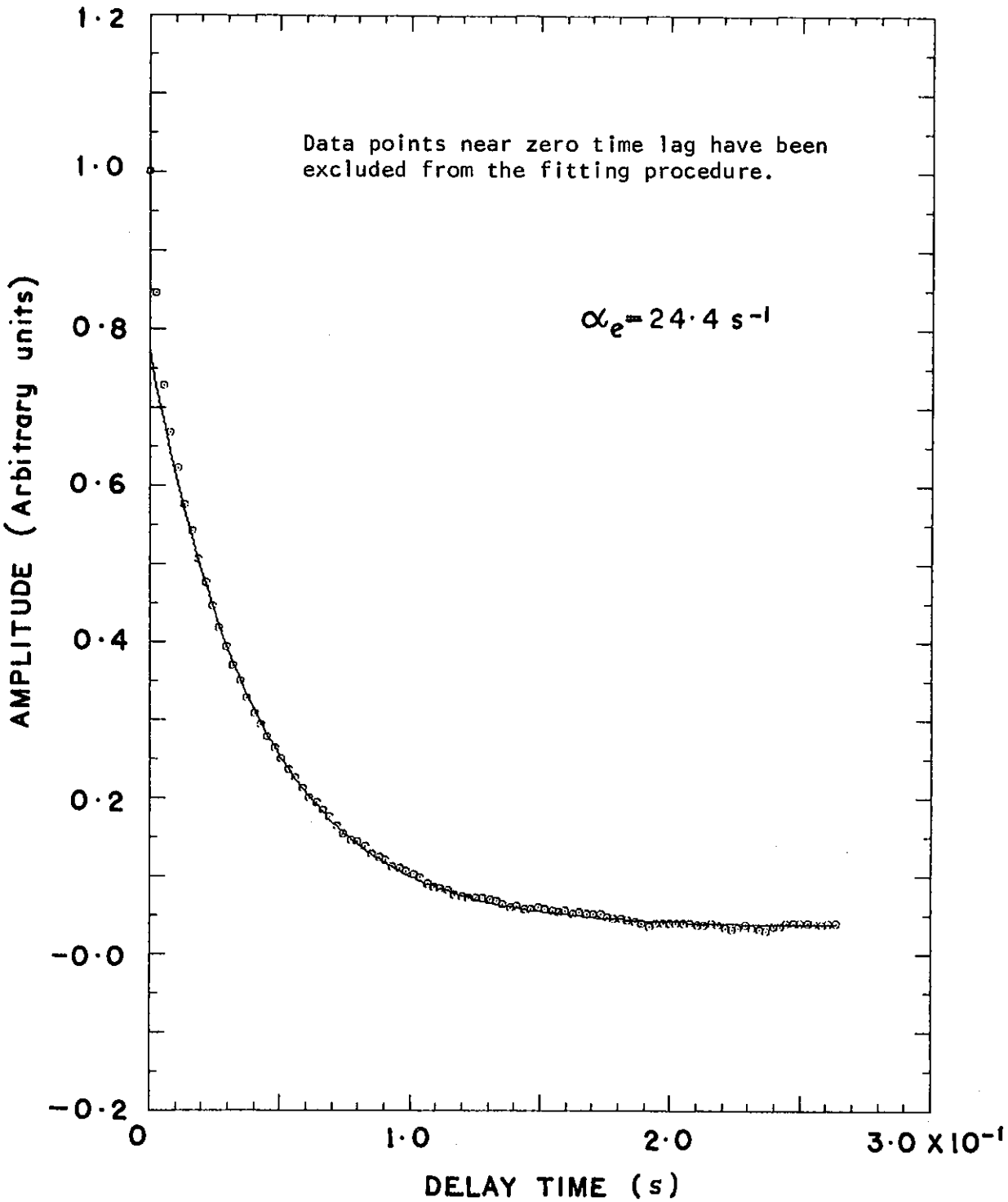

FIGURE 6. AUTO-CORRELOGRAM — M1 ASSEMBLY SHOWING THEORETICAL FIT TO EXPERIMENTAL DATA

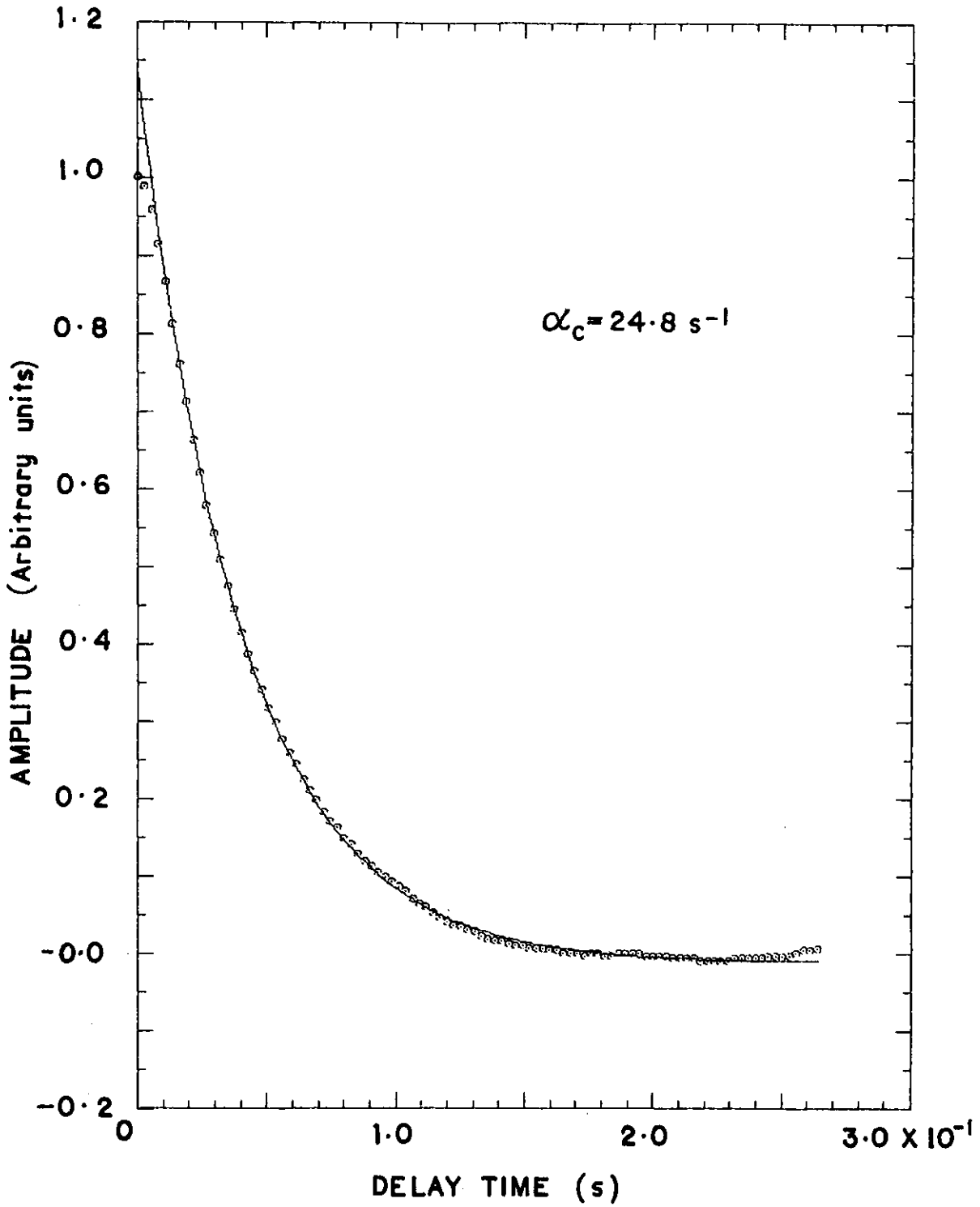

FIGURE 7. CROSS-CORRELOGRAM — M1 ASSEMBLY SHOWING THEORETICAL FIT TO EXPERIMENTAL DATA

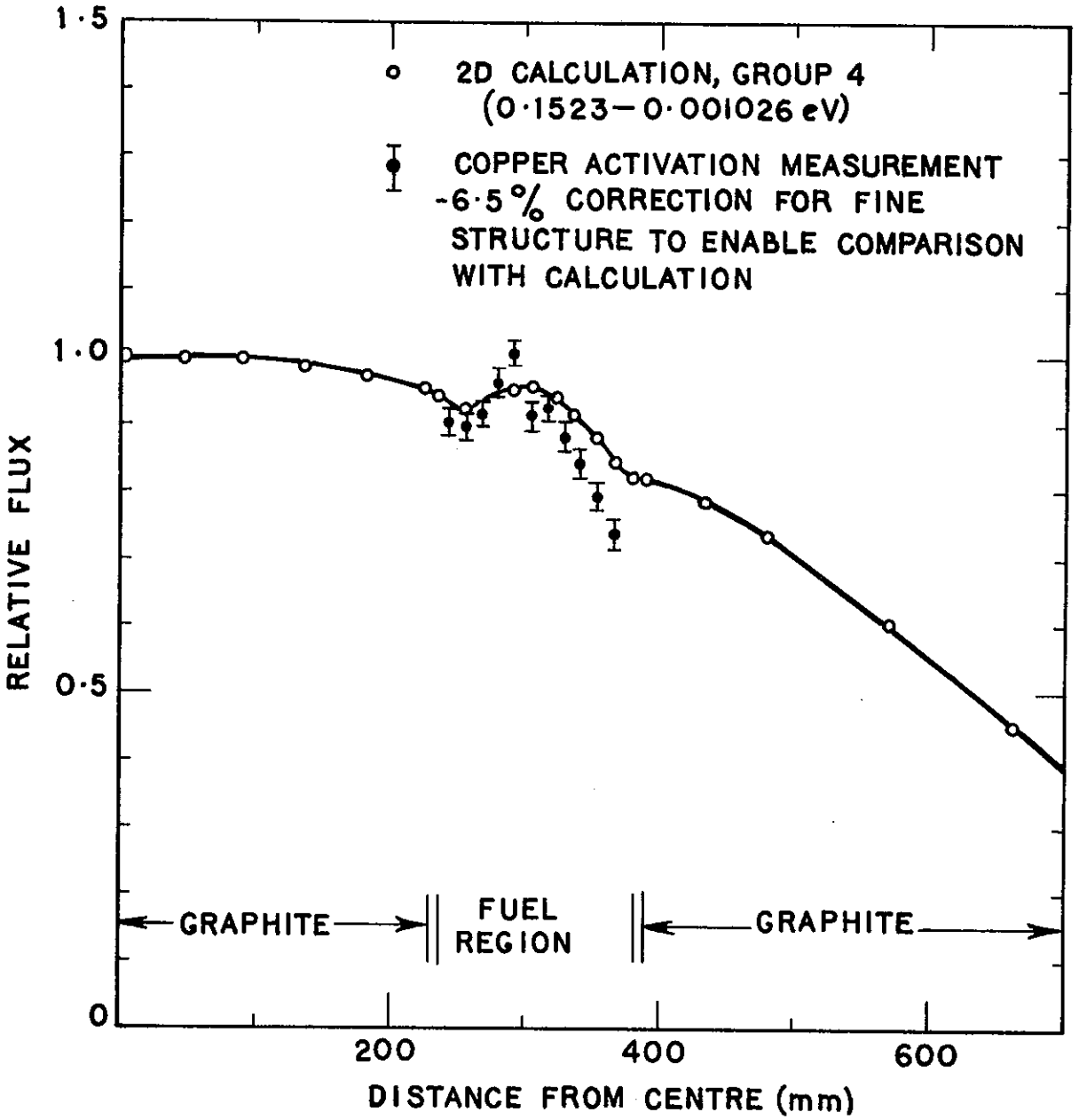

FIGURE 8. THERMAL FLUX DISTRIBUTION FOR MOATA

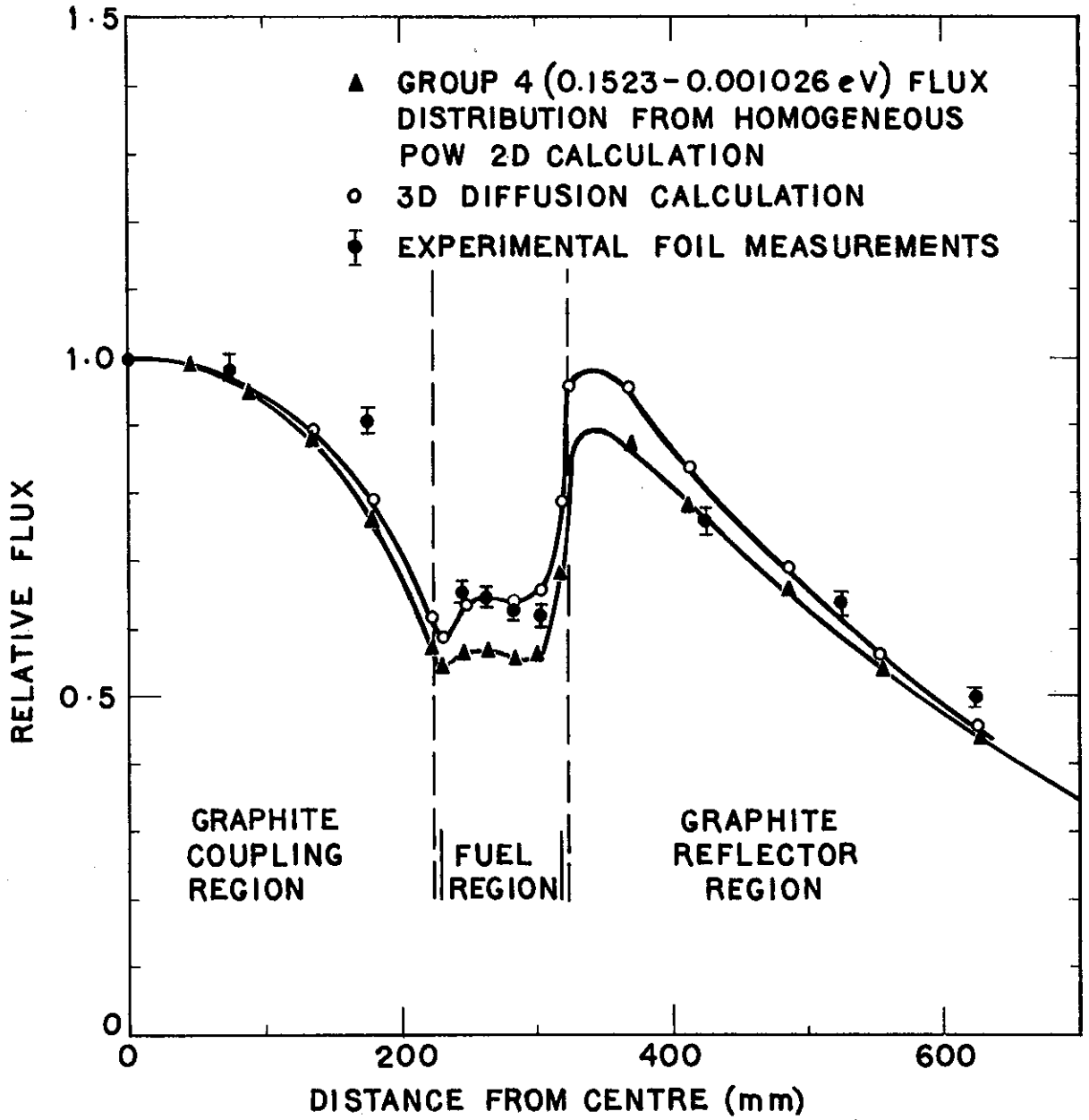

FIGURE 9. THERMAL FLUX DISTRIBUTION FOR M1 ASSEMBLY

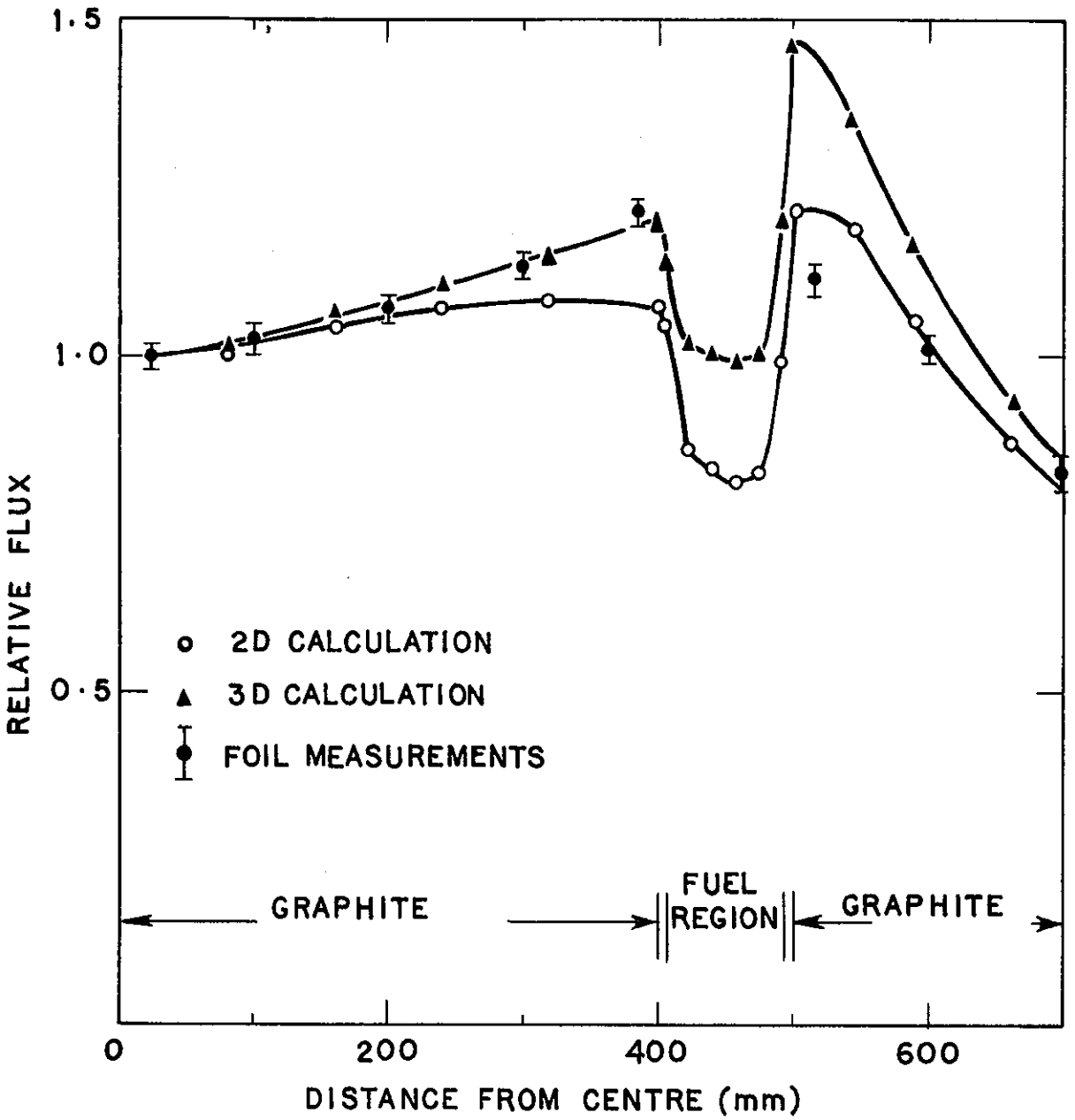

Note : The experimental results at 50 & 60 mm are low probably because of the nearby rod cavity which was neglected in the calculations.

FIGURE 10. THERMAL FLUX DISTRIBUTION FOR M3 ASSEMBLY